Vol 17 No 10, October 2008
1674-1056/2008/17(10)/3856-11

Chinese Physics B

© 2008 Chin. Phys. Soc.
and IOP Publishing Ltd

Characterization of Ag adsorption on TiC(001) substrate: an *ab initio* study*

Ma Shang-Yi(马尚义)[a)b)†] and Wang Shao-Qing(王绍青)[a)]

[a)] *Shenyang National Laboratory for Materials Science, Institute of Metal Research, Chinese Academy of Sciences, Shenyang* 110016, *China*

[b)] *Graduate University of Chinese Academy of Sciences, Beijing* 100049, *China*

(Received 23 September 2007; revised manuscript received 28 May 2008)

Ag adsorptions at 0.25–3 monolayer (ML) coverage on a perfect TiC(001) surface and at 0.25 ML coverage on C vacancy are separately investigated by using the pseudopotential-based density functional theory. The preferential adsorption sites and the adsorption-induced modifications of electronic structures of both the substrate and adsorbate are analysed. Through the analyses of adsorption energy, ideal work of separation, interface distance, projected local density of states, and the difference electron density, the characteristic evolution of the adatom-surface bonding as a function of the amount of deposited silver is studied. The nature of the Ag/TiC bonding changes as the coverage increases from 0.25 to 3 MLs. Unlike physisorption in an Ag/MgO system, polar covalent component contributes to the Ag/TiC interfacial adhesion in most cases, however, for the case of 1–3 ML coverage, an additional electrostatic interaction between the absorption layer and the substrate should be taken into account. The value of ideal work of separation, 1.55 J/m^2, for a 3-ML-thick adlayer accords well with other calculations. The calculations predict that Ag does not wet TiC(001) surface and prefers a three-dimensional growth mode in the absence of kinetic factor. This work reports on a clear site and coverage dependence of the measurable physical parameters, which would benefit the understanding of Ag/TiC(001) interface and the analysis of experimental data.

Keywords: surface adsorption, Ag/TiC interface, DFT calculation, electronic structure
PACC: 7000, 7300, 7320A, 7115A

1. Introduction

As devices continuously shrink in the ultra-large-scale integration (ULSI) industry, Cu resistivity increases substantially in sub-100 nm technology due to edge scattering mechanism, which becomes one of the most critical restrictions on IC performance. It has been shown that Ag is more suitable for ULSI than Cu due to its much higher electrical conductivity in characteristic size below 100 nm.[1,2] Deposition of silver by evaporation, sputtering and electroplating techniques has already been demonstrated by Manepalli *et al* experimentally.[1] Nevertheless, Ag diffuses rapidly in silicon just as Cu does, which can degrade the devices. Since TiC and TiN possess both excellent thermal stability and good chemical stability, they have been recognized as promising candidates for diffusion barrier[3,4] to prevent interdiffusion of Ag in ULSI, especially above 500°C.[5] Therefore, the study on the Ag deposition on TiC and TiN substrates and their interfaces is very significant for ULSI applications.

Understanding the process of metal deposition on substrate at the atomic level is very intriguing in contemporary material science,[6−20] and much attention has been paid to metal adhesion on metal-oxide surfaces, especially on MgO and Al_2O_3 substrates. For the MgO substrate case, alkali metal adsorption on MgO(001) surfaces,[9] Pt deposition on MgO(111) surfaces[10] Ag and Cu adsorption on regular[11−15,41] and defective[16,38] MgO(001) surfaces have been investigated theoretically. For the Al_2O_3 case, the mechanisms for depositing Cu, Ag and Pt on Al_2O_3 surfaces[17−20,42] and the interfaces of Al/Al_2O_3, Ag/Al_2O_3 and Au/Al_2O_3 have also been studied.[21,22] To the best of our knowledge, there is little information about the correlation between structure and property of Ag deposited on TiC substrates. In order to better understand the fundamental process of depositing Ag on TiC(001) surfaces, we study the adsorption energy, ideal work of separation, and electronic structure of Ag/TiC interface evolving with the Ag coverage ranging from 0.25 to 3 MLs and its epi-

*Project supported by the National Basic Research Program of China (Grant No 2006CB605103).
†E-mail: shyma@imr.ac.cn

taxial growth at atomic level in this work. Moreover, the effect of C vacancy on Ag adsorption is also investigated. All these results are compared with those available from other calculations and experiments. We believe that such insights are valuable to microelectronic applications for the Ag/TiC cases.

The remainder of this paper is organized as follows. In Section 2 the model and the computational method used in the paper are described. The major results are presented in Section 3, where the evolutions of interfacial electronic structure and other properties as a function of Ag coverage are described. The wettability and the epitaxial growth mode of Ag on TiC substrates are also discussed in this section. Finally, our results are summarized in Section 4.

2. Computational details

Our electronic structure and total energy calculation are based on the density-functional theory (DFT)[23,24] with the Perdew–Burke–Ernzerhof (PBE)[25] version of generalized gradient approximation. The self-consistent total energy calculations are performed by using the plane wave pseudopotential method implemented in the Quantum-ESPRESSO package,[26] which is used to solve the Kohn–Sham equations through the plane wave expansion for the valence electron density and wavefunctions. The interactions between ions and electrons are described by means of the Vanderbilt ultrasoft pseudopotentials (USPP).[27] Nonlinear core corrections to exchange and correlation are made for all species. The plane wave cutoff is taken to be 40 Ry, which provides a good total energy convergence within 0.0005 Ry/atom. The Brillouin zone is sampled according to the Monkhorst–Pack method.[28] The specific size of the k-point mesh will be given below for each system studied. The total energy of the system is minimized by using the conjugate gradient technique,[29] updating the charge density via the Broyden mixing. Structure relaxations are performed by using the quasi-Newton algorithm and the analytical Hellman–Feynman forces. The structures are optimized until all components of forces are smaller than 0.0004 Ry/atom.

In order to see the accuracy of our computational method, in particular, the pseudopotentials used, Table 1 presents our calculation results of the lattice constant, bulk modulus, and cohesive energy for all the bulk materials of interest here, together with the data available from other calculations and experiments. The bulk calculations are carried out with $8 \times 8 \times 8$ Monkhorst–Pack k-point grids. The lattice constants and bulk modulus are obtained by fitting the Murnaghan equation of state[30] to the total energies calculated from different volumes. The cohesive energies are evaluated as the difference in total energy between bulk ground state and spin-polarized atomic ground state. For the calculation of spin-polarized atomic ground state, a 10 Å (1Å = 0.1 nm) cubic box is used, and the Brillouin zone is sampled at the Γ point only. It is seen from Table that our results are in fairly good agreement with other calculations and measurements . Although some deviations from experimental value can be noticed, the calculations give a reliable and accurate description of the properties of bulk ground state for titanium carbide and silver.

Table 1. A comparison among the present calculations, other calculations and measurements of equilibrium lattice constants α_0, bulk modulus B, and cohesive energies $E_{\rm coh}$ for TiC and Ag.

System	Method	Source	α_0/Å	B/Mbar[b)]	$E_{\rm coh}$/eV
TiC	GGA-PBE	This work	4.356	2.26	7.44
	GGA-PW91	Ref.[40]	4.343	2.47	7.32
	GGA-PW91	Ref.[35]	4.33	2.52	7.3
	Expt	Ref.[35][a)]	4.317	2.4	–
	Expt	Ref.[34]	–	–	7.104
Ag	GGA-PBE	This work	4.206	0.73	2.80
	GGA-PW91	Ref.[40]	4.167	0.89	2.47
	HF	Ref.[31]	4.29	0.72–0.73	2.17
	Expt	Ref.[31][a)]	4.09	1.03	2.97
	Expt	Ref.[32]	–	–	2.97

[a)] quoted from Table 1 in the relevant reference.
[b)] 1 bar = 10^5Pa.

In order to study surface and interface, we use the periodic slab model with two infinite dimensions (X and Y axes) and a finite thickness along the Z-axis, normal to the TiC(001) surface. The vacuum layer of thickness more than 10Å is added to the slabs to minimize the interaction between periodic images of the slabs. To eliminate inherent finite-size effects in the slab model, we check the convergence of the surface energy with respect to the number of atomic layer. Upon attaining to a critical thickness, n, the surface energy will converge to a constant, that is, the two surfaces are ensured to be decoupled by an interior bulk-like region. A 1×1 TiC (001) surface geometry is employed, where each layer contains one Ti atom and one C atom, and the thickness of the slab varies from five to eleven layers. All atoms are allowed to relax with exception of the atoms in the central layer, and $8\times8\times1$ Monkhorst-Pack k-point grids are used. The surface energies are extracted by using the method of linearly fitting the slab energies as suggested by Fiorentini and Mehtfessel.[33] The fitting surface energy is predicted to be about $1.65\,\mathrm{J/m^2}$ and the results for five, seven, nine and eleven layers are 1.66, 1.65, 1.65, and $1.66\,\mathrm{J/m^2}$, respectively. Our calculated surface energy accords well with other density functional theory (DFT) calculation, $1.67\,\mathrm{J/m^2}$.[34] Thus, we believe that five-layer slab warrants an accurate bulklike substrate description for the deposition model. In addition, the TiC (001) surface ripple induced by the difference in displacement between C and Ti atoms is observed. The magnitude of ripple, 0.11Å, is consistent with other calculation, 0.12 Å[35] and experimental result, 0.13 Å.[36]

In summary, we confirm that the computational methods provide an adequate description of the bulk and surface properties, which lends us confidence to carry out the following calculations.

3. Results and discussion

We use a five-layer slab model in our following calculation on the interactions of Ag adatom with the regular and defective TiC(001) surfaces, according to the method discussed in Section 2. The two bottom layers of TiC(001) slab are fixed in the calculation, while one-side Ag coverage on TiC(001) surface is varied from 0.25 to 3 MLs. To reduce computational resources, a series of surface supercells are used for different values of coverage θ of 0.25, 0.5, 1–3 MLs, as depicted in Fig.1. Correspondingly, a series of $4\times4\times1$, $6\times6\times1$, $8\times4\times1$ and $8\times8\times1$ Monkhorst-Pack k-point grids are, respectively, used in Figs.1(a), 1(b), 1(c) and 1(d). Three site-patterns C, Ti, and Hollow (H) sites are considered for the values of coverage θ of 0.25, 0.5 and 1 ML. C-sites and Ti-sites correspond to the sites of top C and Ti atoms, respectively. H-sites refer to the fourfold hollow site, where the Ag atom is above the centre of the square ring. Only C-sites are considered for coverages of 2 and 3 MLs. We ignore the small mismatch (3.4%) between TiC and Ag constants and adjust Ag adlayer to TiC substrate in 1–3 ML adsorption cases. For Ag adatom adsorption on C-vacancy sites, the C-vacancy is modelled as removing one of the four C ions in the 2×2 surface supercell.

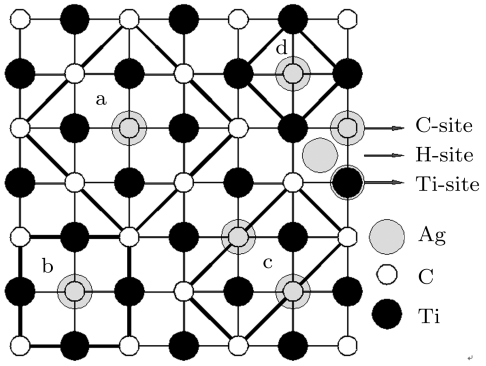


Fig.1. Top view of TiC(001) surface with different surface unit-cells of Ag atom adsorption atop it and patterns of three different adsorption sites C, Ti, and H in the calculation. The surface unit-cells are 2×2 for $\theta=0.25$ MLs (a), a square distribution for $\theta=0.5$ MLs (b), a striped distribution for $\theta=0.5$ MLs (c), and 1×1 for $\theta=1$ ML (d). The unit-cell frames are shown by thick solid lines and only the Ag adsorption above surface C atoms is displayed. The three adsorption site-patterns are C on top of C atoms, Ti on top of Ti atoms, and H above fourfold hollow.

To characterize the adsorption process in detail, two relevant energies are calculated, the adsorption energy per atom, E_{ads}, and the ideal work of separation, W_{sep}. In our calculation, the adsorption energy, E_{ads}, is calculated according to the equation as

$$E_{\mathrm{ads}} = -(E_{\mathrm{Ag/TiC}} - E_{\mathrm{isolated-Ag}} - E_{\mathrm{isolated-TiC}}), \quad (1)$$

where $E_{\mathrm{Ag/TiC}}$ is the total energy of the adsorbate-covered slab, $E_{\mathrm{isolated-Ag}}$ and $E_{\mathrm{isolated-TiC}}$ are the energies for the isolated Ag atom and the clean TiC substrate, respectively. In this way, E_{ads} includes both

the Ag–substrate interaction and the Ag–Ag interaction in the adsorption process. The ideal work of separation, $W_{\rm sep}$ can be calculated as

$$W_{\rm sep} = -(E_{\rm Ag/TiC} - E_{\rm adlayer} - E_{\rm substrate}), \quad (2)$$

where $E_{\rm substrate}$ and $E_{\rm adlayer}$ are the total energies of the same supercell when one of the slabs is kept and the other one is replaced by vacuum. Here, the ideal work of separation $W_{\rm sep}$ accounts for the Ag–substrate interaction only. It shows a direct measure of the interface adhesion and is defined as the energy (the energy per adatom for 0.25–1 ML and per unit-area for 2–3 MLs) required to reversibly cleave the interface into two free surfaces if the plastic and diffusional degrees of freedom are suppressed.[37] Positive $W_{\rm sep}$ value corresponds to the attractive interaction between the substrate and the adlayer. Furthermore, the difference in energy between $E_{\rm ads}$ and $W_{\rm sep}$ can give us a rough estimate of Ag–Ag interaction in the adsorption process. In the following we will present the results concerning the adsorption energy, ideal work of separation and the characteristics of the electronic structure for Ag deposited on the TiC(001) surface.

3.1. $\theta = 0.25$ ML substrate coverage

In the case of 0.25 ML Ag coverage the adsorption energies and the values of ideal work of separation for three surface adsorption sites: C-sites, Ti-sites and H-sites, are evaluated (see Table 2). Compared with the adsorption energy, the direct interaction among Ag adatoms (separated by 6.17 Å) is negligible (about 0.1 eV) and the adatom can be considered as adsorption of isolated Ag atom. The adsorption energies and the values of ideal work of separation are nearly the same.

Table 2. Optimized parameters for different Ag/TiC(001) interfaces. The relevant adsorption positions are shown in Fig.1. $E_{\rm inter}$ is the Ag–Ag interaction. $E_{\rm ads}$, $W_{\rm sep}$ and $E_{\rm inter}$ (from 0.25 to 1 ML) are in units of eV. $W_{\rm sep}$ for 2 and 3 MLs is in units of eV/unit-area. The $W_{\rm sep}$ for 1 ML has the same value in either of the above two units because per unit-area has one adatom for the 1 ML case.

Substrate coverage	Ag atom over	$E_{\rm ads}$	$W_{\rm sep}$	$E_{\rm inter}$	Distance Z-axis/Å		Charge transfer Δq[c)] (e)
					d-atom[a)]	d-plane[b)]	
0.25 ML	C atom	1.49	1.38	0.11	2.149	2.212	–0.23
	Ti atom	0.77	0.64	0.13	2.663	2.590	
	Hollow	1.30	1.24	0.06		2.124	
	C-vacancy	2.55	2.54	0.01	2.839	1.604	
0.5 ML (Square)	C atom	1.51	1.16	0.35	2.174	2.233	–0.15
	Ti atom	0.77	0.34	0.43	2.739	2.674	
	Hollow	1.24	0.85	0.39		2.197	
0.5 ML (Striped)	C atom	1.76	0.76	1.00	2.203	2.257	–0.16
	Ti atom	1.23	0.21	1.01	2.830	2.787	
	Hollow	1.61	0.60	1.01		2.304	
1 ML	C atom	2.11	0.64	1.47	2.267	2.313	–0.12
	Ti atom	1.57	0.10	1.47	3.039	2.993	
	Hollow	1.81	0.34	1.47		2.416	
2 ML	C atom		1.06		2.229[d)]	2.274[d)]	–0.14
3 ML	C atom		0.92		2.264[d)]	2.310[d)]	–0.12

[a)] The distance between the Ag and the adsorption sites.
[b)] The distance between the Ag and the average positions of TiC(001) surface.
[c)] The negative sign indicates charges transferring from Ag to TiC substrate.
[d)] The distance between the first adlayer and TiC substrate.

Table 2 shows that the most preferable sites are C-sites with an adsorption energy of 1.49 eV, which is about 0.72 and 0.19 eV more than those of Ti-sites and H-sites, respectively. The adsorption energy of H-sites is close to an average of the corresponding adsorption energies for the Ag atom, separately, on top of C and Ti sites. The values of ideal work of separation show the same trend of variation in adsorption energy. The Ag–C minimum bond length is 2.149 Å, which is shorter than Ag–Ti minimum bond length (2.663 Å), indicating the strong Ag–C interaction. It is noticeable that the three adsorption geometries are

not equivalent to each other, the Ag–C (Ti, H) distance is not directly representative of the Ag–surface distance. Considering the surface ripple, we define the distance between the adatom and the average surface as the vertical distance between the Ag atom and the surface (d-plane). The d-planes for Ag adsorption for C-sites, Ti-sites and H-sites are 2.212, 2.590 and 2.124 Å respectively.

With the aim of understanding the types of Ag–substrate interaction in three adsorption geometries, the analyses of the electronic local density of states (LDOSs) are presented in Fig.2. The LDOS is projected onto atomic orbitals of the adatoms and surface

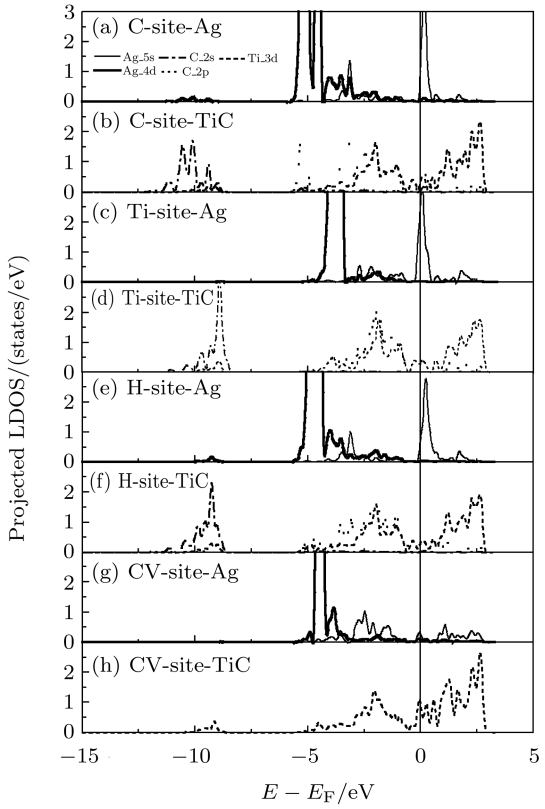


Fig.2. The PLDOSs for 0.25 ML Ag adatoms deposited on C-sites (a), Ti-sites (c), H-sites (e), and C-vacancy sites (g) of TiC(001) surface. The PLDOSs of both Ag (a, c, e, g) and TiC surface atoms (b, d, f, h) are plotted.

atoms. It is seen that the most important feature of the projected local density of states (PLDOSs) is the shift of occupied bonding states on three adsorption sites. The 4d states of Ag deposited on C-sites shift by an energy about 0.7 and 0.2 eV lower than those on Ti-sites and H-sites respectively, which confirms that C-sites are the preferred positions. The PLDOSs of TiC(001) surface provide evidence for both metallic (finite LDOS at E_F) and covalent bondings. The mixing of C 2s electrons with Ti 3d electrons is negligible in lower energy regions, while the strong interaction between C 2p electrons and Ti 3d electrons can be observed at higher energies, representing the main covalent bonding component. In the case of C-site adsorption, the Ag 4d and 5s states highly overlap with surface C 2p states at about –5 and –3 eV, respectively. It reflects the covalent bonding between Ag–C atoms. Similarly, the mixing of Ag 4d, 5s and Ti 3d electrons can also be observed in the plot, although the interaction is very weak. When Ag atoms are deposited on H-sites or Ti-sites, the gravity of Ag 4d band shifts towards higher energies and the overlapping band becomes small compared with that of C-sites adsorption. It is also noticed that when Ag atoms are deposited on C-sites, the Fermi level shifts to the valley of Ag 5s PDOS, which lowers the $N(E_F)$ at Fermi level and leaves more antibonding states unfilled. However, the Fermi level is located in an antibonding region of the Ag 5s states for Ti-site adsorption, that is, the 5s valence electrons occupy all of the bonding states and some of antibonding states, which makes Ti-sites energetically unfavourable.

It is known that a chemical bond is the consequence of the negative charges accumulated in the region between the nuclei to an extent sufficient to balance the nuclear forces of repulsion. The changes in the original atomic density distribution, caused by the formation of the chemical bond, may be extracted and studied directly by the construction of a density difference distribution. The regions of charge increase in the density difference maps are, therefore, the regions to which charges are transferred with respect to the separated atoms to obtain a state of electrostatic equilibrium and hence a chemical bond. From this point of view a density difference map provides us with a picture of the "bond density". The qualitative analysis of charge redistribution accompanied with the Ag adsorption on C-sites, in the cross sections perpendicular to the TiC(001) surface, is illustrated in Fig.3(a). In this case, the densities of the isolated TiC surface and of the isolated Ag adatoms (both with the same geometry as that in the whole system) are subtracted from the density of whole system. To show the charge distribution more clearly, a small contour increment is used. The difference density (or bond density) ($\Delta\rho(r)$) for Ag over C atom shows the electron concentration in the bonding region between Ag and C nuclei. The PLDOS shows the bonding is related to p-d and p-s hybridizations among Ag 4d, 5s and C 2p orbitals.

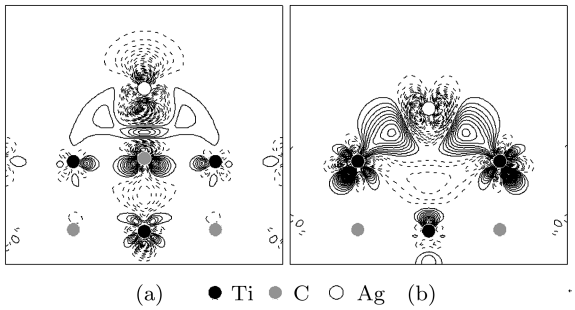


Fig.3. Difference electron density ($\Delta\rho(r)$) maps for a 0.25 ML Ag coverage in the cross-section perpendicular to the (001) interface plane are shown (a) for Ag adsorption on C-sites and (b) for Ag adsorption over C vacancy. Density isolines are drawn from -0.038 to 0.012 e au^{-3} for (a) and from -0.022 to 0.033 e au^{-3} for (b) with an increment of 0.001 e au^{-3} according to their maximum and minimum values. The solid and dashed curves show positive and negative differences densities, respectively.

The Lowdin charge analysis indicates that there exist the 0.37 e charges removed from an Ag adatom with respect to an isolated Ag adatom during the formation of covalent bonds, and the 0.24 and 0.13 e charges removed from 5s and 4d states respectively. However, the C atom is more electronegative than Ag atom and it attracts more electrons than the Ag atom. The consequence of this charge removal is that a polar covalent bond is formed in a direction towards C atom. Lowdin charge analysis shows that there appears an increment of 0.23 e in charge quantity for TiC substrate due to more electrons attracted by C atom. Also observed is the diffuse electron distribution between Ag and Ti atoms, resulting from the weak interaction among Ag 5s, 4d and Ti 3d states. Moreover, one can see that Ag adsorption seems to reduce the electron density between C atoms in the top layer and Ti atoms in the second layer , and more electrons redistribute around the C atoms in the top layer in the x and y directions. From the above discussion it follows that Ag–C polar covalent bonding makes a dominant contribution to the Ag adsorption on C-sites, accompanied with a weak Ag–Ti interaction, which is different from other cases like Ag/oxide metal interfaces in nature. Ag 0.25 and 1ML adsorptions on MgO(001) were studied by Zhukovskii *et al.*[38] They found that chemical bond formation was not important for Ag/MgO(001) perfect interface. At a 0.25 ML coverage, the adsorption energies are 0.23, 0.22, and 0.20 eV for O-sites, Mg-sites and H-sites respectively, which are close to each other for all three adsorption sites due to the partial compensation of the electrostatic attraction for the repulsion of polarized charged Ag adatoms surrounded with surface ions. In the Ag/MgO case, the adsorption is physical in its origin and chemical bond formation is not important in the adsorption process.

When one C atom is removed from the 2×2 surface supercell and one Ag atom is deposited over C vacancy (F_s) centre, we find the adsorption energy increases to 2.55 eV drastically. It is 1.06 eV higher than the adsorption energy for 0.25 ML C-site adsorption of regular surface. The ideal work of separation is nearly the same as the value of adsorption energy and there is hardly any interaction among adatoms (only 0.01 eV per atom). The d-plane reduces to 1.604 Å and the distance between Ag and its nearest neighbouring atoms (four Ti atoms) increases to 2.839 Å. The PLDOSs (Fig.2) show the weak covalent interaction between Ag 5s and Ti 3d electrons, which may contribute to the adsorption, and the negligible interaction between Ag 4d and Ti 3d electrons. The difference electron density distribution (see Fig.3 (b)) depicts that though there appears the electron accumulation between the Ag and its nearest neighbouring coordination atoms (Ti atoms), the electron density is a little diffuse. It is noticeable that when the Ag adsorption takes place over C or Ti sites, there is only a single nearest substrate neighbour (either C or Ti atoms) and four next-nearest substrate ions of opposite type (either Ti or C atoms). The minimum Ag–C and Ag–Ti bonds are 2.149 and 2.663 Å in length, respectively. Thus, when Ag atom is placed over C-sites, the Ti atoms still participate in Ag–Ti bonding besides Ag–C strong interaction, whereas the Ag and C atoms are too far from each other to form a noticeable Ag–C bonding when Ag atom is positioned over Ti-sites. However, for the C vacancy sites, Ag atom interacts with four nearest Ti atoms with an equal distance of 2.839 Å. It shows clearly that the ideal work of separation for C vacancy sites adsorption is about 4 times stronger than that of Ti-sites adsorption. Though the Ag–Ti bonding is not so strong as Ag–C bonding, the interaction between Ag and its four nearest coordination atoms compensates for the longer Ag–Ti bond interaction and makes the C vacancy sites adsorption more energetically favourable, which signifies that the C-vacancy could improve the adhesion of Ag/TiC(001) interface. As reported in experimental study,[39] wettability of TiC by Ag is quite sensitive to TiC stoichiometry. It is known that a decrease in C content can introduce vacancies into the

C sites of TiC. At the most hypostoichiometric composition of $TiC_{0.6}$ Ag shows a dramatic drop in contact angle and undergoes a non-wetting/wetting transition. Other calculation also shows that C vacancies in the first TiC(001) layer have a noticeable effect on the Ag/TiC interface adhesion, about 0.18 J/m^2 enhancement compared with a perfect surface.[40] In an ab initio study of Ag/MgO(001) interface,[41] O vacancies can strongly enhance the metal adhesion to ceramic oxides compared with regular O sites, which is accompanied by a substantial charge transfer (0.32 e) towards Ag adatom as well as a formation of partly covalent Ag–F_s bond across the interface.

3.2. $\theta = 0.5$ ML substrate coverage

At a 0.5 ML coverage there are two different Ag coverage geometries, i.e. a square distribution (sq) (Fig.1(b)) and a striped distribution (st) (Fig.1(c)). In the two adsorption geometries the nearest adatoms are spaced by 4.36 and 3.08 Å for the square distribution and the striped distribution, respectively. When adatoms approach each other, both the interaction among adatoms and the interaction between adatoms and substrate contribute to the adsorption energy in the adsorption process. The adsorption energy in Table 2 increases with coverage increasing form 0.25 to 0.5 MLs. For the 0.5 ML square distribution, the adsorption energy of C-sites increases by only 0.02 eV, whereas the ideal work of separation decreases by about 0.22 eV. The contribution of Ag–Ag interaction to the adsorption energy increases to 0.35 eV. The trend is extremely obvious for the 0.5 ML striped distribution, where the distance between two nearest adatoms is only 3.08 Å, the Ag–Ag interaction becomes a major contribution to the adsorption energy for three adsorption sites. This consists with the fact that new Ag–Ag bonds are created among Ag atoms. One can observe that the enhancements of adsorption energy from Ag–Ag interaction in 0.5 ML striped distribution are nearly equal for the three adsorption sites. Similar to the case of the adsorption at 0.25 ML coverage, the C-sites are also preferable to other sites at the 0.5 ML coverage. In addition, the charge transfer from adatom to substrate for the 0.5 ML C-site square distribution is nearly the same as that of the 0.5 ML striped distribution, the adsorption bondings for the two distributions are also polar covalent for C-sites.

3.3. $\theta = 1$, 2, and 3 ML substrate coverage

At 1 ML coverage one adatom has four equivalent nearest-neighbouring adatoms spaced by 3.08 Å and the new bonds created among adatoms contribute to high adsorption energies for all adsorption sites. The majority of adsorption energies due to adatom interaction all are 1.47 eV for three adsorption sites. At the same time, the values of ideal work of separation decrease to 0.64, 0.10 and 0.34 eV for C-sites, Ti-sites and H-sites, respectively. Similar to the case of partial coverage, C-sites adsorption is more energetically favourable. The optimized d-planes for C-sites, H-sites, and Ti-sites are 2.313, 2.416, and 2.993 Å, respectively, which are longer than that of partial coverage. The C-site characteristic features of 1 ML interfacial bonding can be seen from PLDOSs plotted in Figs.4(a) and 4(b). As expected, the interaction

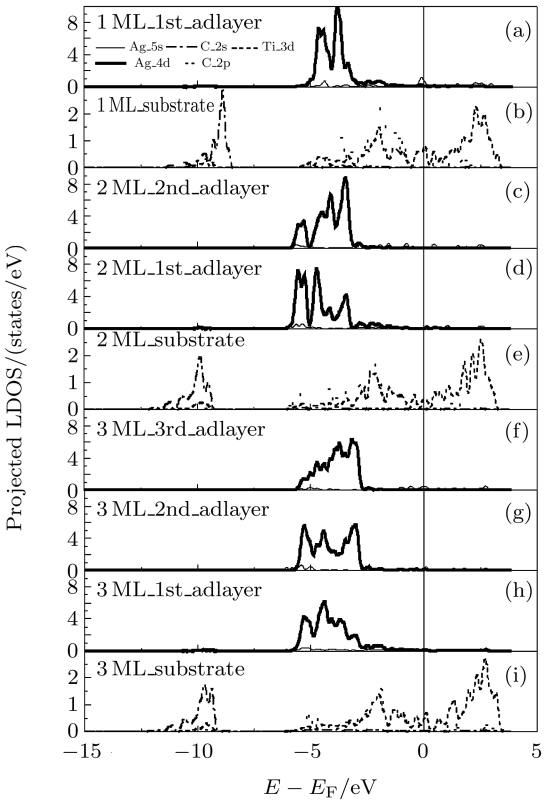


Fig.4. The PLDOSs for 1, 2, and 3 ML Ag adlayers over C-sites of TiC(001) surface. PLDOSs for both Ag adlayer (a, c, d, f, g, h) and substrate surface (b, e, i) are plotted. The first adlayer is close to the interface.

between Ag 4d and C 2p states at –4.5 eV contributes to the covalent component of bonding across the interface mainly. However, the interaction between Ag 5s and C 2p states becomes weak compared with that

in the case of partial coverage. The Lowdin charge analysis also shows that there are only 0.08 e 5s and 0.1 e 4d charge transfers from Ag adatom during the covalent bonding formation, on account of the weaker ideal work of separation. The TiC substrate gains about 0.12 e in charge quantity due to more electrons being attracted by C atom. The mixing among Ti 3d and Ag 4d, 5s electrons can also be observed, but their covalent contributions to the interface bonding are negligible.

The bond density maps for 1 ML Ag coverage show the electron reorganization in an interfacial region for both C and Ti sites clearly (see Figs.5(a) and 5(b)). For the C-site adsorption, the electrons not only concentrate on Ag–C bonds, but also move toward the vacant space above the Ti ion next to the adsorption site. Therefore, it is inferred that the concentrated extra electrons can produce an attractive interaction with the Ti ion underneath, which may also contribute to the interfacial bonding. For Ti-site adsorption, the electron density along Ag–Ti bond is more diffuse.

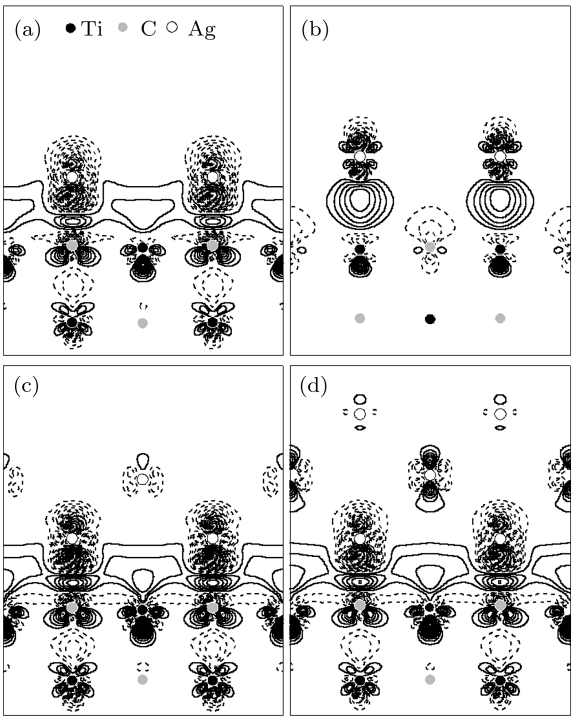


Fig.5. Difference electron density ($\Delta\rho(r)$) maps for 1, 2, and 3 ML Ag coverages in the cross-section perpendicular to the TiC(001) interface plane: (a) for 1 ML Ag positioned over C-sites, (b) for 1 ML Ag positioned over Ti-sites, (c) and (d) for 2 and 3 ML Ag positioned over C-sites, respectively. Density isolines are drawn from -0.027 to 0.014 e au^{-3} for (a), –0.019 to 0.0085 e au^{-3} for (b), –0.038 to 0.022 e au^{-3} for (c), and –0.029 to 0.022 e au^{-3} for (d), with an increment of 0.001 e au^{-3} according to their maximum and minimum values. The solid and dashed curves show positive and negative difference densities, respectively.

At 2 and 3 ML Ag coverages we focus on the most stable configuration, C-site adsorption, based on the preceding discussion. The minimum d-planes are 2.274 and 2.310 Å for 2 and 3 ML coverages, respectively. The values of ideal work of separation for 2 and 3 ML coverages are 1.06 and 0.92 eV/unit-area (about 1.79 and 1.55 J/m^2, respectively). It can be found that the ideal work of separation decreases with coverage increasing from 0.25 to 1 ML (from 1.38 to 0.64 eV/atom for C-sites, the value for the adsorption at 1ML coverage is also 0.64 eV/unit-area) and then increases for the 2 ML coverage (1.06 eV/unit-area), and again declines for the 3ML coverage (0.92 eV/unit-area). The PLDOS indicates that the hybridization between Ag 4d, 5s and C 2p states may contribute to the covalent component for the interface bonding, and the hybridization is achieved to nearly the same extent as that for the case of 1ML adsorption. Again, the Lowdin charge analysis shows that the charge quantity transferred from Ag is the same as that in the case of 1ML coverage. So there must be other factors responsible for enhancing the values of ideal work of separation in the cases of 2 and 3 ML coverages. From the clear charge redistributions for 2 and 3 ML coverages, mapped in Fig.5, one can infer that the values of $W_{\rm sep}$ for 2 and 3 ML coverages are much larger than that for the case of 1 ML coverage, which can be ascribed mainly to the more electrons concentrated in the interfacial Ag adlayer atop surface Ti ions. Studies of full Ag coverage on MgO(001) surface show that the same electron concentration inside silver layers has an attractive interaction with the substrate Mg^{2+} ion underneath,[38,31] thereby causing the Ag/MgO adhesion. For the TiC(100)/Fe(110) system studied by Arya and Carter,[34] the asymptotic value of $W_{\rm sep}$ was predicted to be about 2.56 J/m^2 for a 3-ML-thick coating of TiC on Fe. The value of $W_{\rm sep}$ for TiC(001)/Fe(110) is higher than our value for 3-ML-thick Ag(001)/TiC(001) system due to a significant interaction between C 2p and Fe 3d electrons and somewhat less pronounced mixing between Ti 3d Fe 3d states, the d valence electron of Fe is more delocalized than that of Ag. Our value of $W_{\rm sep}$ for the 3-ML-thick adlayer, 1.55 J/m^2, is close to other Ag(001)/TiC(001) calculation, 1.57 J/m^2,[40] thereby supporting our results. In addition, the electron accu-

mulation is also found between the first adlayer and the second adlayer. The trend is more apparent for the 3 ML coverage, adatoms forming a metallic overlayer with coverage increasing. The Lowdin charge analysis indicates that the value of $W_{\rm sep}$ reducing from 2 to 3 ML may result from the electron delocalization in adlayers and a little weaker interface covalent bonding in 3 ML deposition than that of 2 ML case.

Figure 4 depicts the PLDOSs for different coverages from 1 to 3 adlayers on C-site adsorption. Besides other interfacial features discussed in the preceding section, it is worth noting that the PLDOSs of adlayer and substrate all shift towards lower energies by 0.5 eV from 1 to 2 ML coverage, while the shift between 2 and 3 ML coverage is negligible. With coverage increasing, the broadenings of PLDOSs of adlayer and substrate, induced by the adsorption process, are noticeable. The hybridizations of Ag 5s with C 2p and Ti 3d states become less and less with coverage varying from 1 to 3 MLs, which is in accordance with Lowdin charge analysis. Furthermore, one can note the progressive increasing in Ti 3d C 2p peak mixing around -2.5 eV, indicating that the intraceramic covalent bonding is enhanced with coverage increasing.

To completely understand the electronic structure modification of the Ag adlayer induced by substrate with Ag coverage increasing, the LDOSs of Ag layers in an isolated case and adsorbed on all C-site and C vacancy configurations are plotted in Fig.6. For all coverages, the Ag LDOSs are more or less downshifted for Ag adlayer compared with that for the isolated Ag layer. With respect to the isolated Ag layer, shifts of –2.4, –2.3, –1.6, –1.2, –0.3, and –0.2 eV for 0.25, 0.5 (sq), 0.5 (st), 1, 2, and 3 ML coverages can be found, respectively. The downshift decreases monotonically with coverage varying from 0.25 to 3 MLs. In addition, the shift toward lower energies is seen for the isolated Ag adlayers with layer increasing, indicating further their stabilization. The Ag adatom over C vacancy is more like an isolated atom, with no-split LDOS.

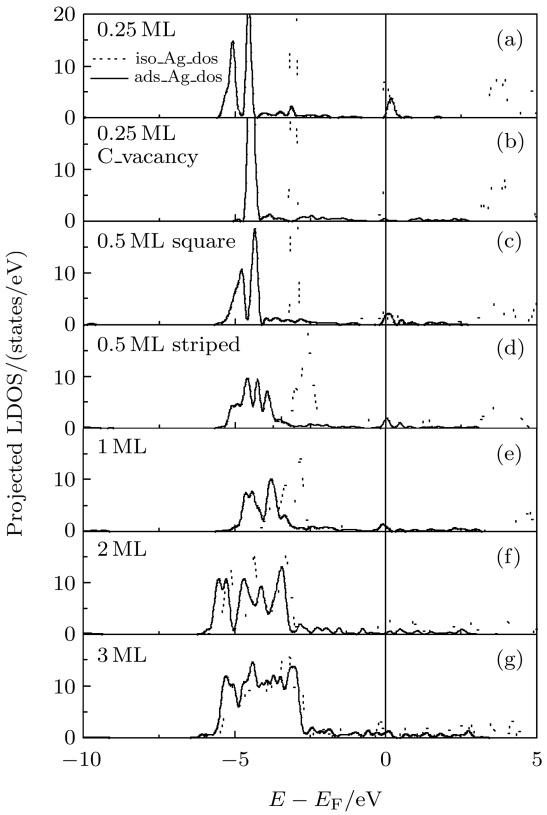


Fig.6. LDOSs of Ag adlayers in an isolated case and adsorbed on all C-site and C vacancy configurations.

3.4. Wettability and growth mode

An important issue involved in the Ag film growth on TiC substrates is the degree of wettability and the growth mode of Ag overlayers. Useful information on growth mode can be obtained from thermodynamic quantities (free energy) or, at zero temperature, in terms of total energy ($E_{\rm t}$) and Born–Haber cycles. With this method, Alexander and Dwight predicted the wettability and growth mode of Cu, Pd and Pt on Al_2O_3 substrate correctly, which accorded well with experiment results.[42] In our case, the relevant calculations (C-sites) are $\Delta_{1\rm sq} = E_{\rm t}(1\text{ML Ag + TiC}) + E_{\rm t}(\text{TiC}) - 2E_{\rm t_sq}(1/2\,\text{ML Ag + TiC})$, $\Delta_2 = E_{\rm t}(2\,\text{ML Ag + TiC}) + E_{\rm t}(\text{TiC}) - 2E_{\rm t}(1\text{ ML Ag + TiC})$, and $\Delta_3 = E_{\rm t}(3\text{ML Ag+TiC}) + 2E_{\rm t}(\text{TiC}) - 3E_{\rm t}(1\text{ML Ag + TiC})$. A positive value of Δ_i indicates that the adsorbate will wet the surface and prefer the layer-by-layer growth mode, and three-dimensional growth otherwise. $\Delta_{1\rm sq}$ is referred to the 0.5 ML square distribution. Our total energy calculations are –0.69, –0.69 and –0.99 eV for $\Delta_{1\rm sq}$, Δ_2 and Δ_3, respectively, which predict that Ag does not wet the TiC(001) surface and prefers three-dimensional growth mode in the absence of kinetic factors. It is worth underlining that the above calculation is a rough estimate of adlayer wettability and growth mode at zero temperature, ignoring other important factors, for example, surface migration and configuration entropy. Nevertheless, it

allows us to obtain the reliable information on wettability and epitaxial growth which could be compared with experimental results. The available reports on wetting experiments with liquid metal on TiC demonstrate the no-wetting behaviour of Ag on TiC surface, with contact angles being 153°[39] and 120°,[43] which verifies the validity of this simplistic approach. Additionally, one can find that the Ag–Ag interaction is stronger than the Ag–TiC interaction, which also implies that Ag can not wet the TiC(001) surface and prefers three-dimensional growth mode.

4. Conclusions

In this work we have analysed the evolution of electronic structure of Ag adsorption at 0.25–3 ML coverage on TiC(001) surface by using the quantum density functional theory-generalized gradient approximation (DFT-GGA) method and also described the features due to Ag–Ag and Ag–substrate interactions . Though there exist some calculation limitations in the adopted model, a few tentative conclusions can be drawn from the present studies.

1) For all Ag coverages on defect-free TiC(001) surface, the adsorption atop C-sites is more energetically preferable than those atop the Ti and H sites. The adsorption energies for the three sites increase monotonically from 0.25 to 1 ML due to the Ag–Ag interaction, whereas the values of ideal work of separation decrease monotonically. Owing to the effect of its high nearest-neighbouring substrate Ti atoms, the adsorption energy and the ideal work of separation for Ag atom positioned over C vacancy are higher than those for any other case, which accounts for the experimental phenomena that the performance of Ag wetting TiC surface is significantly improved on a carbon-deficient titanium carbide substrate.

2) Unlike physisorption in an Ag/MgO system, the interface bonding analysis of Ag/TiC shows that the polar covalent component arising from C 2p and Ag 4d 5s states more or less contributes to interfacial bonding for the most stable configurations from 0.25 to 3 MLs.

3) The nature of the Ag/TiC bonding (for stable configuration, C-sites) changes as the coverage increases from 0.25 to 3 MLs. For a partial coverage, the bonding consists of polar covalent component mainly, whereas for the whole coverage from 1 to 3 MLs, the covalent component becomes less and the contribution of electronic attraction between Ti ion and extra electron concentrated above Ti ion plays an important role gradually.

4) The ideal work of separation is enhanced by the interaction between the substrate Ti ions and the extra electrons accumulated near the interatomic positions of the interfacial Ag layer from 1 to 2 MLs. Owing to more electrons localized between metallic adlayers, the ideal work of separation for the 3 ML coverage slightly decreases in comparison with that for the 2 ML coverage and achieve an asymptotic value, $1.55\,\mathrm{J/m^2}$. There appears no noticeable change in interfacial distance from 1 to 3 ML coverage.

5) By analysing the adsorption-induced modifications of the electronic structure of the adsorbate, it is found that the LDOS shifts towards low energies generally when the substrate coverage increases, indicating that the configuration is further stabilized. The energy calculations predict that Ag atom cannot wet the TiC(001) surface and prefers the three-dimensional growth mode in the absence of kinetic factor.

References

[1] Manepalli R, Stepniak F, Bidstrup-Allen S A and Kohl P 1999 *IEEE Trans. Adv. Pack.* **22** 4

[2] Hauder M, Gstötner J, Hansch W and Schmitt Landsiedel D 2001 *Appl. Phys. Lett.* **78** 838

[3] Eizenberg M and Brener R 1984 *J. Appl. Phys.* **55** 3799

[4] Wang S J, Tsai H Y and Sun S C 2001 *J. Electrochem. Soc.* **148** C563

[5] Yoganand S N, Raghuveer M S, Jagannadham K, Wu L and Karoui A 2002 *Appl. Phys. Lett.* **80** 79

[6] Ma L, Wang J G and Wei S Y 2004 *Chin. Phys.* **13** 85

[7] Yan H and Zhu X Y 2005 *Chin. Phys.* **14** 2083

[8] Lu Z S, Luo G X and Yang Z X 2007 *Acta Phys. Sin.* **56** 5352 (in Chinese)

[9] James A S and John E J 2000 *J. Chem. Phys.* **112** 3014

[10] Goniakowski J and Noguera C 1999 *Phys. Rev.* B **60** 16120

[11] Fuks D, Dorfman S and Kotomin E A 2000 *Phys. Rev. Lett.* **85** 4333

[12] Fuks D, Dorfman S, Zhukovskii Y F, Kotomin E A and Stoneham A M 2002 *Surf. Sci.* **499** 24

[13] Herschend B, Hermansson K, Alfredsson M, Zhukovskii Y F, Kotomin E A and Jacobs P W M 2003 *J. Phys. Chem.* B **107** 11893

[14] Ferrari A M 2004 *Chem. Phys. Lett.* **400** 541

[15] Zhukosvkii Y F, Kotomin E A, Fuks D and Dorfman S 2004 *Superlattices Microstruct.* **36** 63

[16] Zhukosvkii Y F, Kotomin E A, Jacobs P WM and Stoneham A M 2000 *Phys. Rev. Lett.* **84** 1256
[17] Fdez J S and Hernandez N C 2005 *Phys. Rev. Lett.* **94** 016104
[18] Chatterjee A, Niwa S and Mizukami F 2005 *J. Mol. Graphics Modell.* **23** 447
[19] Zhukovskii Y F, Kotomin E A, Herschend B, Hermansson K and Jacobs P W M 2002 *Surf. Sci.* **513** 343
[20] Verdozzi C, Jennison D R, Schultz P A and Sears M P 1999 *Phys. Rev. Lett.* **82** 799
[21] Feng J W, Zhang W Q and Wan J 2005 *Phys. Rev.* B **72** 115423
[22] Smith J R and Zhang W 2000 *Acta Mater.* **48** 4395
[23] Hohenberg P and Kohn W 1964 *Phys. Rev.* **136** B864
[24] Kohn W and Sham L 1965 *Phys. Rev.* **140** A1133
[25] Perdew J P, Burke K and Ernzerhof M 1996 *Phys. Rev. Lett.* **77** 3865
[26] Baroni S, Dal Corso A, de Gironcoli S, Giannozzi P, Cavazzoni C, Ballabio G, Scandolo S, Chiarotti G, Focher P, Pasquarello A, Laasonen K, Trave A, Car R, Marzari N and Kokalj A http://www.pwscf.org
[27] Vanderbilt D 1990 *Phys. Rev.* B **41** 7892
[28] Monkhorst H J and Pack J D 1976 *Phys. Rev.* B **13** 5188
[29] Teter M P, Payne M C and Allan D C 1989 *Phys. Rev.* B **40** 12255
[30] Murnaghan F D 1944 *Proc. Natl. Acad. Sci.* U.S.A. **30** 244
[31] groi M, Pisani C and Busso M 2001 *Thin Solid Films* **400** 64
[32] schneidner K A 1964 *J. Solid State Phys.* **16** 276
[33] Fiorentini V and Methfessel M 1996 *J. Phys.*: *Condens. Matter* **8** 6525
[34] Arya A and Carter E A 2003 *J. Chem. Phys.* **118** 8982
[35] Dudiy S V and Lundqvist B I 2001 *Phys. Rev.* B **64** 045403
[36] Tagawa M, Kawasaki T, Oshima C, Otani S, Edamoto K and Nagashima A 2002 *Surf. Sci.* **517** 59
[37] Finnis M W 1996 *J. Phys.*: *Condens. Matter* **8** 5811
[38] Zhukovskii Y F, Kotomin E A, Fuks D, Dorfman S and Gordon A. 2001 *Surf. Sci.* **482-485** 66
[39] Xiao P and Derby B 1996 *Acta Mater.* **44** 307
[40] Dudiy S V and Lundqvist B I 2004 *Phys. Rev.* B **69** 125421
[41] Zhukovskii Y F, Kotomin E A and Borstel G 2004 *Vacuum* **74** 235
[42] Alexander B and Dwight R J 1999 *Phys. Rev. Lett.* **82** 4050
[43] Frage N, Froumin N and Dariel M P 2002 *Acta Mater.* **50** 237